Published in final edited form as:

*Kidney Int*. 2019 July ; 96(1): 67–79. doi:10.1016/j.kint.2019.01.009.

# Differential contribution of C5aR and C5b-9 pathways to renal thrombic microangiopathy and macrovascular thrombosis in mice carrying an atypical hemolytic syndrome-related factor H mutation.

**Yoshiyasu Ueda**[1], **Takashi Miwa**[1], **Daisuke Ito**[1], **Hangsoo Kim**[1], **Sayaka Sato**[1], **Damodar Gullipalli**[1], **Lin Zhou**[1], **Madhu Golla**[1], **Delu Song**[2], **Joshua L. Dunaief**[2], **Matthew Palmer**[3], **Wen-Chao Song**[1]

[1]Department of Systems Pharmacology and Translational Therapeutics, Perelman School of 12 Medicine, University of Pennsylvania, Philadelphia, PA 19104

[2]Department of Ophthalmology, Perelman School of 12 Medicine, University of Pennsylvania, Philadelphia, PA 19104

[3]Department of Pathology and Laboratory Medicine, Perelman School of 12 Medicine, University of Pennsylvania, Philadelphia, PA 19104

## Abstract

Atypical hemolytic uremic syndrome (aHUS) is a form of thrombotic microangiopathy (TMA) caused by dysregulated complement activation. Clinically, aHUS is effectively treated by an anti-C5 mAb but whether the disease is mediated by the C5a receptor (C5aR) or C5b-9 pathway, or both, is unknown. Here we address this in FHR/R mice which developed complement-mediated TMA as well as macrovascular thrombosis caused by an aHUS-related factor H point mutation (mouse W1206R, corresponding to human W1183R). C5 deficiency and anti- C5 mAb treatment blocked all disease manifestations in FHR/R mice. C5aR1 gene deficiency prevented macrovascular thrombosis in various organs but did not improve survival or reduce renal TMA. Conversely, C6 or C9 deficiency significantly improved survival and markedly diminished renal TMA but did not prevent macrovascular thrombosis. Interestingly, as they aged both FHR/R C6−/− and FHR/R C9−/− mice developed glomerular disease reminiscent of C3 glomerulonephritis. Thus, C5aR and C5b-9 pathways drove different aspects of disease in FHR/R mice with the C5aR pathway being responsible for macrovascular thrombosis and chronic inflammatory injury while

*To whom requests for reprint should be addressed at:* Wen-Chao Song Ph.D. University of Pennsylvania School of Medicine, Room 1254 BRBII/III, 421 Curie Blvd., Philadelphia, PA 19104, Tel: 215-573-6641, Fax: 215-746-8941, songwe@pennmedicine.upenn.edu.

Disclosure

WCS has received research funding from Alexion Pharmaceuticals, Inc. All other author(s) have no competing financial interests to declare.

Supplementary Methods

Supplementary information is available at Kidney International's website

the C5b-9 pathway causing renal TMA. Our data provide new understanding of the pathogenesis of complement-mediated TMA and macrovascular thrombosis in FHR/R mice and suggest that C5 blockade is more effective for the treatment of aHUS than selectively targeting the C5aR or C5b-9 pathway alone.

## Graphical Abstract

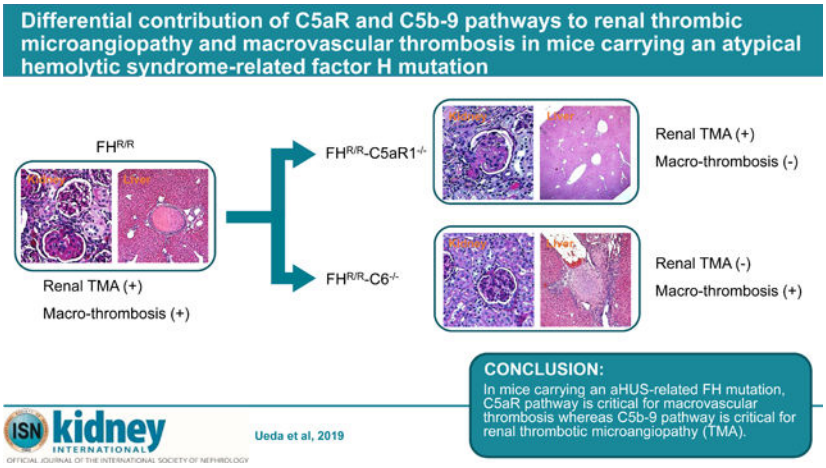


### Keywords

Complement; atypical hemolytic uremic syndrome (aHUS); thrombotic microangiopathy (TMA); C5a receptor (C5aR); membrane attack complex (MAC)

## Introduction

Atypical hemolytic uremic syndrome (aHUS) is a disease characterized by the triad of thrombocytopenia, microangiopathic hemolytic anemia and kidney injury.[1, 2] Before the advent of anti-complement therapy, it had a poor prognosis with high mortality, and end-stage renal disease developed in majority of the patients.[1, 2] We now know that most aHUS cases are caused by dysregulated alternative pathway (AP) complement activation, and many aHUS-related complement gene mutations have been identified.[1–4] Some of them are loss of function mutations in plasma or cell surface-anchored complement regulatory proteins such as factor H (FH), factor I and membrane cofactor protein, while others are gain of function mutations in C3 or factor B that render the self-amplifying C3 convertase C3bBb resistant to regulation.[5–12] In other cases, autoantibodies to complement factor H have been linked to aHUS disease.[13–16] Regardless of the nature of complement defects, a shared consequence is inadequate control of AP complement activation on host cells, most critically endothelial cells and platelets.[17] This leads to complement-mediated tissue injury at vulnerable sites such as the kidney glomeruli to produce thrombotic microangiopathy (TMA), a hallmark pathology of aHUS.

Treatment for aHUS had been limited to plasma infusion/exchange before an anti-C5 monoclonal antibody (Eculizumab) was approved.[18–20] Eculizumab dramatically improved

patient outcomes and is now the standard therapy. Despite the effectiveness of anti-C5 treatment, the pathogenesis of aHUS remains incompletely understood. Activation of C5 produces two split products, C5a and C5b. C5a is a potent proinflammatory mediator that acts by binding to its cognate G protein coupled receptor (C5a receptor, C5aR) on leukocytes.[21] C5b initiates the formation of C5b-9, the membrane attack complex (MAC), by sequentially binding to C6, C7, C8 and C9.[21] The MAC then inserts into and causes the disruption of cell membranes, leading to cell lysis and death.[21] Presently little is known about the respective roles of C5a/C5aR and MAC pathways in the pathogenesis of aHUS, and whether selectively inhibiting one or the other pathway may be sufficient to treat aHUS. A more selective drug targeting either the C5a/C5aR or the MAC pathway, if effective, would be more desirable than Eculizumab in managing aHUS as it would leave the other effector pathway intact for host defense and may also provide more dosing convenience. Indeed, to our knowledge, at least one such effort is being made to evaluate the efficacy of an orally active C5aR antagonist, CCX-168, for the treatment of aHUS.[22]

In the present study, we have dissected the respective roles of C5aR and C5b-9 pathways in the pathogenesis of renal TMA and macrovascular thrombosis in mice carrying an aHUS-related FH mutation. We previously created a homozygous FH mutant mouse ($FH^{R/R}$) by introducing a point mutation W1206R which corresponds to W1183R mutation in certain aHUS patients.[23, 24] $FH^{R/R}$ mice developed aHUS-like pathologies including thrombocytopenia, hemolytic anemia and renal failure. They also displayed a systemic thrombophilia phenotype with formation of large-vessel thrombi in multiple organs, and many developed ischemic brain injury and retinopathy due to blood vessel occlusion in the brain and retina.[25] By crossing $FH^{R/R}$ mice with mice deficient in C5, C5aR1, C6 or C9, we confirmed the key role of C5 in the pathogenesis of renal TMA and revealed that both C5aR and C5b-9 pathways were important but they contributed to different aspects of $FH^{R/R}$ pathologies.

## Results

### C5 deficiency or anti-C5 mAb treatment in $FH^{R/R}$ mice prevented renal TMA and macro-vessel thrombosis

We previously showed that mice carrying a homozygous FH point mutation W1206R ($FH^{R/R}$) developed severe aHUS-like disease including thrombocytopenia, hemolytic anemia and renal disease and approximately half died by 30 weeks of age.[25] They also developed macro-vessel thrombi in multiple organs including the liver, spleen and lung and about 30 % had neurological symptoms consistent with stroke.[25] To assess the role of terminal complement pathway in this model, we crossed $FH^{R/R}$ mice with $C5^{-/-}$ mice and generated $FH^{R/R}$ $C5^{-/-}$ mice. As shown in Figure 1a, approximately 50 % of $FH^{R/R}$ mice (n = 58) generated from double heterozygous breeders died by 20 weeks of age whereas all $FH^{R/R}$ $C5^{-/-}$ littermates (n = 52) were alive at the same time point. Complete blood count (CBC) analysis showed low platelet counts and hemoglobin (Hb) levels in $FH^{R/R}$ but not $FH^{R/R}$ $C5^{-/-}$ or $FH^{W/W}$ (wild-type, WT) mice (Figure 1b, c). Likewise, blood urea nitrogen (BUN) measurement showed age-dependent increase in $FH^{R/R}$ but not $FH^{R/R}$ $C5^{-/-}$ or $FH^{W/W}$ mice (Figure 1d). On histology, $FH^{R/R}$ mice showed TMA features in the kidney, including

mesangial expansion, narrowing of capillary lumens and micro-thrombi, whereas $FH^{R/R}$ $C5^{-/-}$ mice showed no signs of TMA, even at 40 weeks of age (Figure 2a and Table 1). Additionally, significant fibrin staining was found in the glomeruli of $FH^{R/R}$ mice but not $FH^{R/R}$ $C5^{-/-}$ or $FH^{W/W}$ mice (Figure 2c, f). As expected, both $FH^{R/R}$ and $FH^{R/R}$ $C5^{-/-}$ mice exhibited granular C3 staining in glomeruli, but none was detected in $FH^{W/W}$ mouse glomeruli (Figure 2b, e). As we observed before,[25] the majority (80%) of $FH^{R/R}$ mice in the current experiment had large-vessel thrombi in the liver, and 8%, 16%, 16% and 40% also had thrombi detected in the heart, brain, lung and spleen, respectively, but no thrombi were detected in any of the organs of $FH^{R/R}$ $C5^{-/-}$ or $FH^{W/W}$ mice (Figure 2d and Table 2). These data indicated that C5 is critical for aHUS disease pathogenesis in $FH^{R/R}$ mice. Dependency of disease pathogenesis on C5 was further confirmed by treating $FH^{R/R}$ mice with an anti-C5 mAb (Table1 and 2, Supplementary Figure S1).

## C5aR1 deficiency did not reduce mortality or TMA severity in $FH^{R/R}$ mice

To dissect the role of C5a/C5aR effector pathway in the disease pathogenesis of $FH^{R/R}$ mice, we crossed $FH^{R/R}$ mice with mice deficient in C5aR1 and monitored disease development in $FH^{R/R}$ $C5aR1^{-/-}$ mice. We found that C5aR1 deficiency did not improve survival rate of $FH^{R/R}$ mice, as close to 70 % of $FH^{R/R}$ $C5aR1^{-/-}$ mice died by 20 weeks of age as compared to 50% mortality in $FH^{R/R}$ mice (Figure 3a). C5aR1 deficiency also failed to rescue $FH^{R/R}$ mice from developing thrombocytopenia, hemolytic anemia and renal disease. As in $FH^{R/R}$ mice, platelet counts and Hb levels in $FH^{R/R}$ $C5aR1^{-/-}$ mice were significantly lower than in $FH^{W/W}$ mice, and there was an age-dependent increase in BUN levels in $FH^{R/R}$ $C5aR1^{-/-}$ mice, which was suggestive of progressive renal disease (Figure 3b–d). On light and immunofluorescence microscopy, $FH^{R/R}$ $C5aR1^{-/-}$ mice showed similar renal TMA characteristics to $FH^{R/R}$ mice and comparable C3 and fibrin immunofluorescence staining was observed in the glomeruli of these two strains of mice (Figure 4 and Table 1). Likewise, on electron microscopy, $FH^{W/W}$ mouse glomeruli showed normal basement membrane and foot processes but both $FH^{R/R}$ and $FH^{R/R}$ $C5aR1^{-/-}$ mice had typical TMA features including sub-endothelial space expansion (yellow arrow) and endothelial swelling without dense deposit (Figure 4d). Additionally, we found $FH^{R/R}$ $C5aR1^{-/-}$ mice, like $FH^{R/R}$ mice, had similarly elevated plasma von Willebrand factor (vWF) level (Supplementary Figure S2).

## C6 or C9 deficiency reduced mortality and ameliorated renal TMA in $FH^{R/R}$ mice

To assess the role of C5b-9 in aHUS, we first generated a $C6^{-/-}$ mouse strain from a commercially available C6 gene targeted embryonic stem cell line. Lack of C6 protein and hemolytic activity in $C6^{-/-}$ mice was confirmed by Western blot and red blood cell lysis test, respectively (supplementary Figure S3). We also characterized a commercially sourced $C9^{-/-}$ mouse and confirmed that it lacked plasma C9 with greatly reduced (especially in female mice), but not absent, hemolytic activity (supplementary Figure S4). We crossed $FH^{R/R}$ mice with $C6^{-/-}$ or $C9^{-/-}$ mice and studied the resultant $FH^{R/R}$ $C6^{-/-}$ and $FH^{R/R}$ $C9^{-/-}$ mice. In contrast to the lack of beneficial effect of C5aR1 deficiency on survival, C6 or C9 deficiency significantly reduced mortality of $FH^{R/R}$ mice (Figure 3a). It was apparent, however, that blocking C5b-9 by C6 or C9 deletion was not sufficient to fully rescue $FH^{R/R}$ mice from disease, as low-rate premature death still occurred with $FH^{R/R}$ $C6^{-/-}$ and $FH^{R/R}$

$C9^{-/-}$ mice (Figure 3a), and thrombocytopenia and hemolytic anemia persisted (Figure 3b, c). On the other hand, 10-week old $FH^{R/R}$ $C6^{-/-}$ and $FH^{R/R}$ $C9^{-/-}$ mice had significantly reduced BUN levels compared with age-matched $FH^{R/R}$ mice (Figure 3d), suggesting that they had sustained less renal injury. While not excluding extravascular hemolysis as a potential mechanism for the anemia, we detected no steady state C3-opsonization on circulating RBCs in $FH^{R/R}$ $C6^{-/-}$ or $FH^{R/R}$ $C9^{-/-}$ mice (Supplementary Figure S5) nor in $FH^{R/R}$ mice (data not shown).

Amelioration of renal TMA in $FH^{R/R}$ $C6^{-/-}$ and $FH^{R/R}$ $C9^{-/-}$ mice was confirmed on renal histology. By light microscopy, we detected no TMA features such as expanded matrix and endothelial swelling, micro-thrombi, glomerular sclerosis or arteriolar hyalinosis in the glomeruli of 10-week old $FH^{R/R}$ $C6^{-/-}$ mice (Figure 5a and Table 1). Glomeruli of 10-week old $FH^{R/R}$ $C9^{-/-}$ mice were not TMA-free, but they showed significantly less pathology than $FH^{R/R}$ mice (Figure 5b and Table 1). Furthermore, no fibrin, and significantly less C3, deposition was observed in 10-week old $FH^{R/R}$ $C6^{-/-}$ and $FH^{R/R}$ $C9^{-/-}$ mouse glomeruli than in $FH^{R/R}$ mouse glomeruli (Figure 5c–f and supplementary Figure S6).

## Renal disease progressed with aging in $FH^{R/R}$ $C6^{-/-}$ and $FH^{R/R}$ $C9^{-/-}$ mice

With $FH^{R/R}$ $C9^{-/-}$ mice, we observed a marked age-dependent progression of renal TMA. Compared with 10-week old mice, 20- and 40-week old $FH^{R/R}$ $C9^{-/-}$ mice had a much higher percentage of glomeruli showing expanded matrix, endothelial swelling, micro-thrombi, arteriolar hyalinosis and deposition of fibrin (Figure 5b, f, Table 1 and Supplementary Figure S6b). Other than a moderate increase in arteriolar hyalinosis in 40-week old mice, age-dependent renal TMA progression was not observed in $FH^{R/R}$ $C6^{-/-}$ mice (Figure 5a, Table 1 and Supplementary Figure S6b). Interestingly, we found that both $FH^{R/R}$ $C6^{-/-}$ mice (40-week old) and $FH^{R/R}$ $C9^{-/-}$ mice (10-week and older) developed significant glomerular hypercellularity (Figure 5a, b and Table 1). Granular C3 staining in mesangial and capillary lesions was also positive and accompanied the hypercellularity phenotype (Figure 5c, d and Supplemental Figure S6a). On electron microscopy, changes that are characteristic of both TMA (e.g. endothelial swelling) and C3 glomerulonephritis (e.g. electron-dense deposits in sub-endothelial and mesangial lesions) were detected in the glomeruli of $FH^{R/R}$ $C6^{-/-}$ (40-week old) and $FH^{R/R}$ $C9^{-/-}$ mice (20-week and older) (Figure 5g, h). Notably, glomerular hypercellularity or dense deposit was not observed in 40-week old $FH^{R/R}$ $C5^{-/-}$ mice (Table 1 and Supplementary Figure S7). However, the age-dependent development of renal pathology in either $FH^{R/R}$ $C6^{-/-}$ or $FH^{R/R}$ $C9^{-/-}$ mice was not associated with significant elevation of BUN (Supplementary Figure S8). These results suggested that C6 deficiency offered more protection than C9 deficiency from renal TMA, but in both strains the remaining C5a/C5aR pathways may have driven a glomerular pathology with features of C3 glomerulonephritis as the mice aged.

## C5aR1 but not C6 or C9 deficiency prevented macro-vessel thrombosis in $FH^{R/R}$ mice

Contrasting to the lack of an effect of C5aR1 deficiency on survival and renal TMA, we found that C5aR1 deficiency, but not C6 or C9 deficiency, prevented macro-vessel thrombosis in $FH^{R/R}$ mice (Figure 6a, Table 1 and 2). As in $FH^{R/R}$ mice, macro-vessel thrombi were detected in the kidney, liver, lung and spleen of a significant percentage of

$FH^{R/R}$ $C6^{-/-}$ and $FH^{R/R}$ $C9^{-/-}$ mice, but none was present in the organs of $FH^{R/R}$ $C5aR1^{-/-}$ mice (Table 1 and 2). To better understand macro-vessel thrombosis and its dependency on C5aR, we examined large vessel thrombi by immunofluorescence staining for presence of the coagulation proteins fibrin, vWF and tissue factor, and of cellular components such as platelets (CD41), neutrophils (Ly6G) and other leukocytes including T lymphocytes (CD45). Both liver macro-thrombi and kidney micro-thrombi in $FH^{R/R}$ mice were rich in fibrin and vWF, and they stained strongly for the platelet marker CD41, moderately for the neutrophil marker Ly6G, weakly for CD45 and negatively for tissue factor (Figure 6b and Supplementary Figure S9). Liver thrombi in $FH^{R/R}$ $C6^{-/-}$ and $FH^{R/R}$ $C9^{-/-}$ mice had similar patterns of staining for fibrin, vWF, CD41 and Ly6G (Supplementary Figure S10). These data suggested that platelets and neutrophils, but not lymphocytes, may be implicated in the formation of fibrin- and vWF-rich thrombi detected in various organs of $FH^{R/R}$, FHR/R $C6^{-/-}$ and FHR/R $C9^{-/-}$ mice.

In an attempt to understand the differential contribution of C5aR and C5b-9 pathways to renal TMA and macro-vessel thrombosis in $FH^{R/R}$ mice, we stained C5b-9 deposition and C5aR1 expression in the glomeruli, and in kidney and liver macro-vessel thrombi of WT, $FH^{R/R}$ and $FH^{R/R}$ $C9^{-/-}$ mice. We detected C9 deposition both in the glomerular capillaries and in the macro-vessel thrombi of $FH^{R/R}$ but not WT or $FH^{R/R}$ $C9^{-/-}$ mice (Supplementary Figure S11). This result implied that C5b-9 was generated both in the glomerular microvasculature and in the macro-vessel thrombi but it played a critical role only in the pathogenesis of renal TMA. In contrast, we detected specific staining of C5aR1 only in macro-vessel thrombi but not in kidney glomeruli of either healthy or diseased mice (Supplementary Figure S12). In addition, tissue-specific deletion of C5aR1 from myeloid lineage cells of $FH^{R/R}$ mice (achieved by crossing a C5aR1 floxed mouse with lysozyme-Cre transgenic mouse) was sufficient to rescue the macro-vessel thrombosis phenotype (Sato et al, unpublished result), suggesting that the phenotype was driven by C5aR1 activation on myeloid-lineage leukocytes.

## Discussion

It is now well established that complement dysregulation is the underlying cause in the majority of aHUS cases.[1–4] The proven efficacy of Eculizumab, a humanized anti-C5 mAb, in the treatment of aHUS has suggested that C5 and the terminal complement pathway play a critical role in aHUS pathogenesis.[26] However, it is still not clear whether aHUS is primarily mediated by the C5a/C5aR or the C5b-9 pathway, or both. Understanding how terminal complement activation causes aHUS is critical for optimizing aHUS diagnosis and treatment. For example, by selectively targeting only the pathogenic arm of the terminal pathway, new anti-complement drugs may be developed that are potentially more specific and easier to dose but less costly and with fewer immune-compromising side effects.

In the present study, we have evaluated the pathogenic role of C5a/C5aR and C5b-9 pathways in mice that carry an aHUS-related FH mutation.[25] $FH^{R/R}$ mice developed characteristic renal TMA as well as macro-vessel thrombosis in multiple organs. The latter is not usually observed in human patients but is likely a more severe phenotype brought about by homozygosity of the FH mutation. Our study here confirmed the critical role of

C5 in aHUS and validated plasma C5 inhibition as an effective therapeutic strategy for this disease. It also revealed that both C5a/C5aR and C5b-9 pathways are important for disease pathogenesis in the $FH^{R/R}$ mouse model but these pathways drove different pathology. We found that C5aR1 but not C5b-9 was critical for macro-vessel thrombosis, whereas renal TMA was mainly caused by C5b-9. The fact that $FH^{R/R}$ $C6^{-/-}$ and $FH^{R/R}$ $C9^{-/-}$ mice, but not $FH^{R/R}$ $C5aR1^{-/-}$ mice, had significantly improved 20-week survival rate suggested that C5b-9-mediated TMA was the major cause of premature mortality in $FH^{R/R}$ mice. Interestingly, neither C5aR1 deficiency nor C6 or C9 deficiency rescued thrombocytopenia and hemolytic anemia of $FH^{R/R}$ mice. This finding implied that thrombocytopenia in these mice was caused by platelet consumption from C5aR-dependent macro-vessel thrombosis as well as TMA-related capillary thrombosis in the kidney and other tissues. Hemolytic anemia in aHUS is thought to result from red blood cell fragmentation as they pass through the narrowed lumen of glomerular capillaries at high velocity, as evidenced by the presence of schistocytes in patients' blood.[27] Persistence of anemia in $FH^{R/R}$ $C6^{-/-}$ and $FH^{R/R}$ $C9^{-/-}$ mice in which TMA was prevented or significantly ameliorated implied that a different or additional mechanisms may account for this phenotype in $FH^{R/R}$ mice.

While both C6 and C9 are obligatory components of C5b-9, the membrane attack complex, we noted a clear difference in the phenotypes of $FH^{R/R}$ $C6^{-/-}$ and $FH^{R/R}$ $C9^{-/-}$ mice. We found that $FH^{R/R}$ $C6^{-/-}$ mice were largely resistant to renal TMA, whereas significant renal TMA developed in aged (20- and 40-week old) $FH^{R/R}$ $C9^{-/-}$ mice. This finding suggested that C5b-had significant MAC activity and was capable of damaging renal vascular endothelial cells to cause TMA. Indeed, we found that serum from $C9^{-/-}$ but not $C6^{-/-}$ mice retained some hemolytic activity in an *in vitro* red blood cell lysis test (Supplementary Figure S4c). That C9 is dispensable in MAC-mediated cellular injury was also noted in a previous study that compared the lytic activities of normal and C9-depleted human sera.[28] Nevertheless, in both instances, C5b-9 was clearly more effective than C5b-8 as a membrane attack complex, as C9 deficiency significantly reduced cell lysis in the previous study[28] and substantially protected $FH^{R/R}$ mice from premature death and renal TMA in the current study.

Of interest, we observed a prominent glomerular hypercellularity phenotype in $FH^{R/R}$ $C9^{-/-}$ mice and in FHR/R $C6^{-/-}$ mice as the latter aged. Furthermore, C3 staining and electron-dense deposits were detected in mesangial and capillary lesions and accompanied the glomerular hypercellularity phenotype. Notably, such a phenotype was not observed in aged $FH^{R/R}$ $C5^{-/-}$ mice. These findings suggested that C5a/C5aR-mediated complement pathways had the potential to drive a C3 glomerulonephritis-like pathology in these FH mutant mice. In $FH^{R/R}$ mice, severe TMA may have masked the development potential of such pathological changes but in the context of C6 or C9 deficiency, amelioration of TMA and a longer lifespan enabled such a pathogenic mechanism to manifest itself. The fact that significant glomerular hypercellularity was present in 10-week and older $FH^{R/R}$ $C9^{-/-}$ mice but only in 40-week old $FH^{R/R}$ $C6^{-/-}$ mice implied that C5b-8 complex may also have contributed to its pathogenesis.

Mechanistically, C5b-9 may have contributed to renal TMA by stimulating platelet activation as well as causing endothelial injury and activation in the glomerular

microvasculature. How C5aR1 activation led to formation of large-vessel thrombosis remains to be elucidated. C5aR1 is most abundantly expressed on neutrophils and moderately on monocytes[21, 29] and preliminary result from C5aR1 conditional knockout mice showed C5aR1 expression on myeloid-lineage leukocytes was critical for macro-vessel thrombosis. By immunofluorescence staining, we detected the presence of both platelets and neutrophils in liver and kidney thrombi. It is possible that C5aR-mediated neutrophil and monocyte activation promoted the formation of platelet-leukocyte aggregates which in turn initiated thrombotic reactions in large blood vessels of the hypercoagulable $FH^{R/R}$ mice. Platelet-leukocyte aggregates are known to be a risk factor and marker for prothrombotic disorders in humans.[30–32] In addition, $FH^{R/R}$ mice had elevated blood vWF levels which, when combined with increased platelet sensitivity to aggregation as a result of complement dysregulation on the platelet surface, may have predisposed these mice to a hypercoagulable state. It has been proposed that release of tissue factor from C5a/C5aR-activated leukocytes may promote the extrinsic pathway of coagulation.[33, 34] However, we detected no tissue factor staining in the large-vessel thrombi of $FH^{R/R}$ mice.

In summary, using the recently created $FH^{R/R}$ mouse and mice deficient in C5aR and C5b-9 effector pathways, we have provided new understanding of the pathogenesis of renal TMA and macro-vessel thrombosis caused by an aHUS-related FH mutation. Overall, our data support the conclusion that both downstream pathways of C5 activation contribute to aHUS pathogenesis, and that C5 blockade can be expected to be more effective for the treatment of aHUS than selectively targeting C5aR or C5b-9 pathway alone.

## Methods

### Mice

The generation of $FH^{R/R}$ mice, source of other knockout mice and the generation of various double knockout mice are described in Supplementary Methods.

### Survival curve

Survival curves were plotted using the GraphPad Prism program (La Jolla, CA) as described previously.[35]

### Measurement of blood urea nitrogen (BUN) and complete blood count (CBC) analysis

BUN was measured using serum and urea nitrogen reagents (Sigma-Aldrich, St Louis, MO) as described previously.[36] CBC was measured using an automated hematology analyzer (XT-2000iV, Sysmex) at the Translational Core Laboratory of the Children's Hospital of Philadelphia.[25]

### Histological analysis

Kidney tissue sectioning, histology and immunofluorescence staining and pathology scoring were performed by following similar protocols as described previously [25]. Experimental details are provided in the Supplementary Methods section.

### Anti-C5 mAb treatment

$FH^{R/R}$ mice were treated with a mouse anti-mouse C5 mAb (clone: BB5.1) or an isotype control mAb (MOPC 31C) as described.[37, 38] The mAbs were purified from mouse ascites produced by Cocalico Biologicals, Inc. (Reamstown, PA) and dialyzed against phosphate-buffered saline.

$FH^{R/R}$ mice were treated twice weekly (1 mg/mouse, intraperitoneal injection) starting at 4 weeks of age. Mice were treated for a total of 8 weeks.

### Expression of recombinant mouse C6 and C9

Mouse C6 and C9 cDNAs were obtained from Origene (Rockville, MD) and cloned into the pCAGGS-mFHSP-mFH19/20–8×His plasmid at NotI and SmaI sites [39]. Each construct was transiently transfected into HEK cells (American Type Culture Collection). At 48 hours after transfection, cells were switched to serum-free medium and cultured for two more days. The cell culture medium was then collected and recombinant protein was purified by $Ni^{2+}$-chelate chromatography (QIAGEN, Valencia, CA).

### Generation of rabbit polyclonal antibodies against mouse C6 and C9

Polyclonal rabbit anti-mouse C6 and C9 Abs were generated by Cocalico Biologicals Inc (Reamstown, PA) using purified mouse C6 and C9 as immunogens (300 μg and 400 μg/rabbit in 4 immunizations), respectively.

### Hemolysis assay

$DAF^{-/-}Crry^{-/-}C3^{-/-}$ mouse [40] erythrocytes ($1.6 \times 10^7$ cells/reaction) were mixed with anti-mouse FH monoclonal antibody (clone: 7–1, 150 μg/ml) and 50 % mouse serum diluted in $Mg^{2+}$-EGTA-GVB in a final volume of 50 μl. EDTA-serum was used as a negative control. Cells were incubated for 40 min at 37 °C, after which cold EDTA-PBS was added to stop the reaction. Reactions were centrifuged and the supernatant OD values were measured at 405 nm. Percentage hemolysis was calculated by dividing the $OD_{405}$ value with that of a sample in which total hemolysis was induced by hypotonic shock.

### Statistics

Survival curves were plotted was analyzed using the GraphPad Prism program (La Jolla, CA) and analyzed by Mantel-Haeszel log-rank test. CBC data, BUN data, and fluorescence intensity results were expressed as mean ± SD. Results were analyzed using the unpaired 2-tailed Student's *t* test or one-way ANOVA. Analyses were performed using the GraphPad Prism program (La Jolla, CA). Statistical significance was accepted for *P* less than 0.05.

## Supplementary Material

Refer to Web version on PubMed Central for supplementary material.

## Acknowledgment

This work is supported by NIH grants AI117410, AI44970, AI085596 and EY023709. We are grateful to the services provided by the Transgenic and Chimeric Mouse Facility and the Electron Microscopy Core of the

Perelman School of Medicine, University of Pennsylvania for chimeric mouse production and electron microscopy, respectively, and the Clinical and Translational Research Center of the Children's Hospital of Philadelphia for mouse CBC analysis.

This work is supported by NIH grants AI117410, AI44970, AI085596 and EY023709.

## References

1. Noris M, Remuzzi G. Atypical hemolytic-uremic syndrome. The New England journal of medicine 2009; 361: 1676–1687. [PubMed: 19846853]
2. Nester CM, Barbour T, de Cordoba SR, et al. Atypical aHUS: State of the art. Molecular immunology 2015; 67: 31–42. [PubMed: 25843230]
3. Kavanagh D, Richards A, Atkinson J. Complement regulatory genes and hemolytic uremic syndromes. Annual review of medicine 2008; 59: 293–309.
4. Kavanagh D, Goodship TH, Richards A. Atypical hemolytic uremic syndrome. Seminars in nephrology 2013; 33: 508–530. [PubMed: 24161037]
5. Richards A, Buddles MR, Donne RL, et al. Factor H mutations in hemolytic uremic syndrome cluster in exons 18–20, a domain important for host cell recognition. Am J Hum Genet 2001; 68: 485–490. [PubMed: 11170896]
6. Perez-Caballero D, Gonzalez-Rubio C, Gallardo ME, et al. Clustering of missense mutations in the C-terminal region of factor H in atypical hemolytic uremic syndrome. Am J Hum Genet 2001; 68: 478–484. [PubMed: 11170895]
7. Noris M, Brioschi S, Caprioli J, et al. Familial haemolytic uraemic syndrome and an MCP mutation. Lancet 2003; 362: 1542–1547. [PubMed: 14615110]
8. Richards A, Kemp EJ, Liszewski MK, et al. Mutations in human complement regulator, membrane cofactor protein (CD46), predispose to development of familial hemolytic uremic syndrome. Proceedings of the National Academy of Sciences of the United States of America 2003; 100: 12966–12971. [PubMed: 14566051]
9. Fremeaux-Bacchi V, Dragon-Durey MA, Blouin J, et al. Complement factor I: a susceptibility gene for atypical haemolytic uraemic syndrome. J Med Genet 2004; 41: e84. [PubMed: 15173250]
10. Kavanagh D, Kemp EJ, Mayland E, et al. Mutations in complement factor I predispose to development of atypical hemolytic uremic syndrome. J Am Soc Nephrol 2005; 16: 2150–2155. [PubMed: 15917334]
11. Goicoechea de Jorge E, Harris CL, Esparza-Gordillo J, et al. Gain-of-function mutations in complement factor B are associated with atypical hemolytic uremic syndrome. Proceedings of the National Academy of Sciences of the United States of America 2007; 104: 240–245. [PubMed: 17182750]
12. Fremeaux-Bacchi V, Miller EC, Liszewski MK, et al. Mutations in complement C3 predispose to development of atypical hemolytic uremic syndrome. Blood 2008; 112: 4948–4952. [PubMed: 18796626]
13. Noris M, Mele C, Remuzzi G. Podocyte dysfunction in atypical haemolytic uraemic syndrome. Nature reviews Nephrology 2015; 11: 245–252. [PubMed: 25599621]
14. Dragon-Durey MA, Loirat C, Cloarec S, et al. Anti-Factor H autoantibodies associated with atypical hemolytic uremic syndrome. Journal of the American Society of Nephrology : JASN 2005; 16: 555–563. [PubMed: 15590760]
15. Kavanagh D, Pappworth IY, Anderson H, et al. Factor I autoantibodies in patients with atypical hemolytic uremic syndrome: disease-associated or an epiphenomenon? Clinical journal of the American Society of Nephrology : CJASN 2012; 7: 417–426. [PubMed: 22223611]
16. Jozsi M, Reuter S, Nozal P, et al. Autoantibodies to complement components in C3 glomerulopathy and atypical hemolytic uremic syndrome. Immunology letters 2014; 160: 163–171. [PubMed: 24491679]
17. Hyvarinen S, Meri S, Jokiranta TS. Disturbed sialic acid recognition on endothelial cells and platelets in complement attack causes atypical hemolytic uremic syndrome. Blood 2016; 127: 2701–2710. [PubMed: 27006390]

18. Loirat C, Fremeaux-Bacchi V. Atypical hemolytic uremic syndrome. Orphanet J Rare Dis 2011; 6: 60. [PubMed: 21902819]
19. Tsai HM. Thrombotic thrombocytopenic purpura and the atypical hemolytic uremic syndrome: an update. Hematology/oncology clinics of North America 2013; 27: 565–584. [PubMed: 23714312]
20. Kaplan BS, Ruebner RL, Spinale JM, et al. Current treatment of atypical hemolytic uremic syndrome. Intractable Rare Dis Res 2014; 3: 34–45. [PubMed: 25343125]
21. Dunkelberger JR, Song WC. Complement and its role in innate and adaptive immune responses. Cell research 2010; 20: 34–50. [PubMed: 20010915]
22. Bekker P, Dairaghi D, Seitz L, et al. Characterization of Pharmacologic and Pharmacokinetic Properties of CCX168, a Potent and Selective Orally Administered Complement 5a Receptor Inhibitor, Based on Preclinical Evaluation and Randomized Phase 1 Clinical Study. PLoS One 2016; 11: e0164646.
23. Remuzzi G, Ruggenenti P, Codazzi D, et al. Combined kidney and liver transplantation for familial haemolytic uraemic syndrome. Lancet 2002; 359: 1671–1672. [PubMed: 12020532]
24. Ferreira VP, Herbert AP, Cortes C, et al. The binding of factor H to a complex of physiological polyanions and C3b on cells is impaired in atypical hemolytic uremic syndrome. J Immunol 2009; 182: 7009–7018. [PubMed: 19454698]
25. Ueda Y, Mohammed I, Song D, et al. Murine systemic thrombophilia and hemolytic uremic syndrome from a factor H point mutation. Blood 2017; 129: 1184–1196. [PubMed: 28057640]
26. Zuber J, Fakhouri F, Roumenina LT, et al. Use of eculizumab for atypical haemolytic uraemic syndrome and C3 glomerulopathies. Nature reviews Nephrology 2012; 8: 643–657. [PubMed: 23026949]
27. Zini G, d'Onofrio G, Briggs C, et al. ICSH recommendations for identification, diagnostic value, and quantitation of schistocytes. Int J Lab Hematol 2012; 34: 107–116. [PubMed: 22081912]
28. Morgan BP, Imagawa DK, Dankert JR, et al. Complement lysis of U937, a nucleated mammalian cell line in the absence of C9: effect of C9 on C5b-8 mediated cell lysis. J Immunol 1986; 136: 3402–3406. [PubMed: 3514758]
29. Dunkelberger J, Zhou L, Miwa T, et al. C5aR expression in a novel GFP reporter gene knockin mouse: implications for the mechanism of action of C5aR signaling in T cell immunity. J Immunol 2012; 188: 4032–4042. [PubMed: 22430734]
30. von Hundelshausen P, Weber C. Platelets as immune cells: bridging inflammation and cardiovascular disease. Circ Res 2007; 100: 27–40. [PubMed: 17204662]
31. Zarbock A, Polanowska-Grabowska RK, Ley K. Platelet-neutrophil-interactions: linking hemostasis and inflammation. Blood Rev 2007; 21: 99–111. [PubMed: 16987572]
32. May AE, Seizer P, Gawaz M. Platelets: inflammatory firebugs of vascular walls. Arterioscler Thromb Vasc Biol 2008; 28: s5–10. [PubMed: 18174454]
33. Ritis K, Doumas M, Mastellos D, et al. A novel C5a receptor-tissue factor cross-talk in neutrophils links innate immunity to coagulation pathways. J Immunol 2006; 177: 4794–4802. [PubMed: 16982920]
34. Redecha P, Tilley R, Tencati M, et al. Tissue factor: a link between C5a and neutrophil activation in antiphospholipid antibody induced fetal injury. Blood 2007; 110: 2423–2431. [PubMed: 17536017]
35. Lesher AM, Zhou L, Kimura Y, et al. Combination of factor H mutation and properdin deficiency causes severe C3 glomerulonephritis. Journal of the American Society of Nephrology : JASN 2013; 24: 53–65. [PubMed: 23204401]
36. Yamada K, Miwa T, Liu J, et al. Critical protection from renal ischemia reperfusion injury by CD55 and CD59. J Immunol 2004; 172: 3869–3875. [PubMed: 15004194]
37. Frei Y, Lambris JD, Stockinger B. Generation of a monoclonal antibody to mouse C5 application in an ELISA assay for detection of anti-C5 antibodies. Mol Cell Probes 1987; 1: 141–149. [PubMed: 3453897]
38. Williams AL, Gullipalli D, Ueda Y, et al. C5 inhibition prevents renal failure in a mouse model of lethal C3 glomerulopathy. Kidney international 2017; 91: 1386–1397. [PubMed: 28139294]

39. Barata L, Miwa T, Sato S, et al. Deletion of Crry and DAF on murine platelets stimulates thrombopoiesis and increases factor H-dependent resistance of peripheral platelets to complement attack. J Immunol 2013; 190: 2886–2895. [PubMed: 23390291]

40. Molina H, Miwa T, Zhou L, et al. Complement-mediated clearance of erythrocytes: mechanism and delineation of the regulatory roles of Crry and DAF. Decay-accelerating factor. Blood 2002; 100: 4544–4549. [PubMed: 12393518]

### Translational Statement

Although aHUS is effectively treated by Soliris, a humanized anti-C5 mAb, it is not known whether the disease is caused by C5a-mediated inflammatory injury or C5b-9-dependnet tissue damage. A better understanding of this question will help to guide the development of new anti-complement drugs that may be more selective with less side effects. For example, a C5a receptor antagonist (CCX-168) has been tested in phase II clinical trials as a potential therapy for aHUS. However, data presented in this study have shown that both the C5a receptor and C5b-9 pathways are pathogenic in a murine model of renal TMA and macrovascular thrombosis caused by an aHUS-related factor H mutation. We conclude that drugs inhibiting C5 such as Soliris may provide more efficacy clinically in managing aHUS than other therapeutic agents that selectively target only one of the two downstream pathways beyond C5 activation.

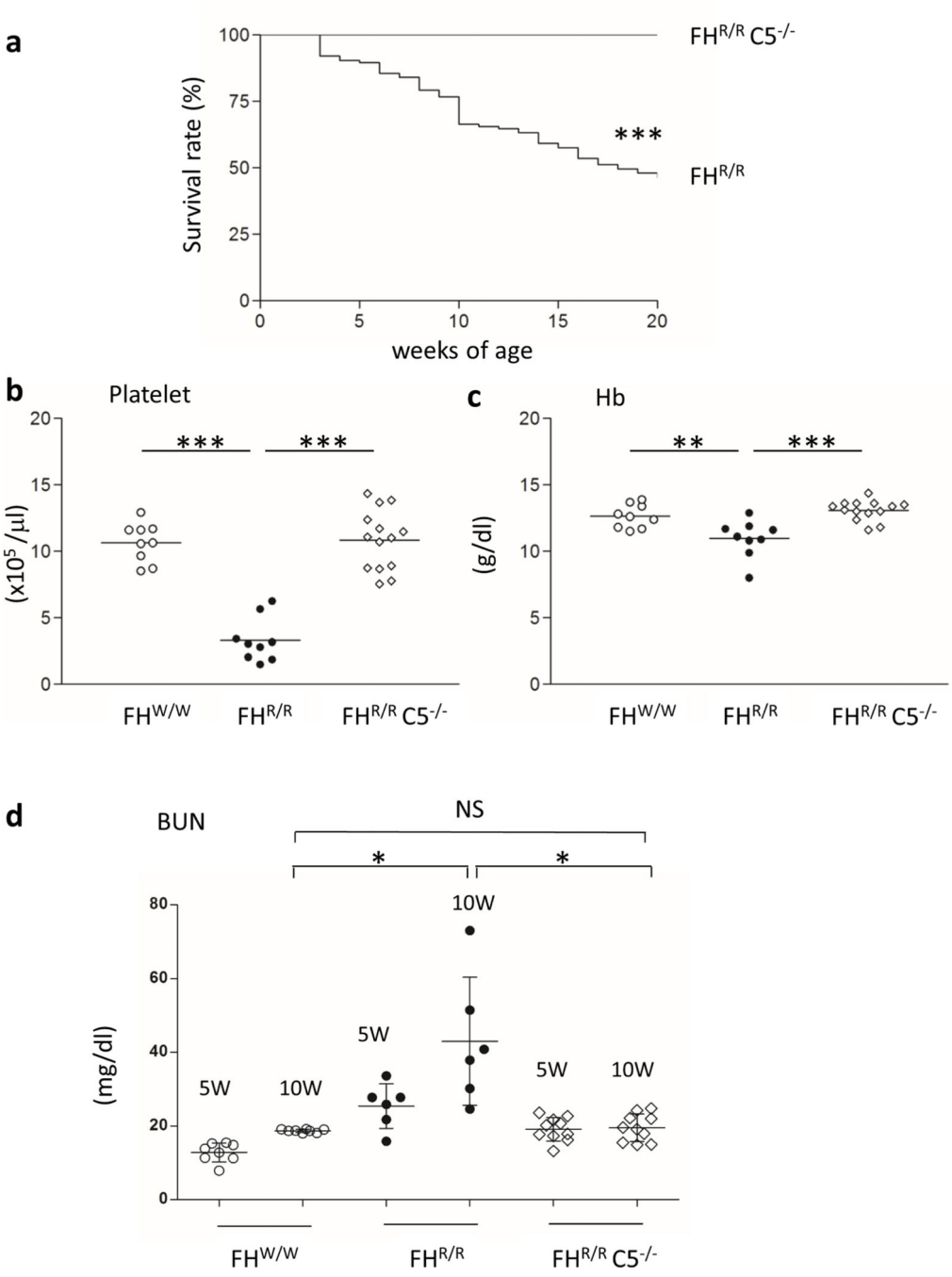


**Figure 1. C5 deficiency protected FH$^{R/R}$ mice from aHUS and premature death.**

(a) Survival curves of FH$^{R/R}$ (n = 58) and FH$^{R/R}$ C5$^{-/-}$ (n = 52) mice by 20 weeks of age. (b-c) FH$^{R/R}$ mice (n = 9) exhibited thrombocytopenia (b) and anemia (c), whereas FH$^{R/R}$ C5$^{-/-}$ mice (n = 14) had normal platelet counts and hemoglobin (Hb) levels similar to wild-type (FH$^{W/W}$) mice (n = 9). (d) Blood urea nitrogen (BUN) level in 10-week old FH$^{R/R}$ mice (n = 6) was higher than that of age-matched FH$^{W/W}$ (n=8) or FH$^{R/R}$ C5$^{-/-}$ (n=10) mice, but there was no difference between 10-week old FH$^{W/W}$ and FH$^{R/R}$ C5$^{-/-}$ mice. In b-c, scatter plots represent individual mice (4–20 weeks of age), and horizontal bars through

the plots indicate average values. *$P < 0.05$, **$P < 0.01$, ***$P < 0.001$. Mantel-Haenszel log-rank test for panel a, one-way ANOVA for panels b-d.

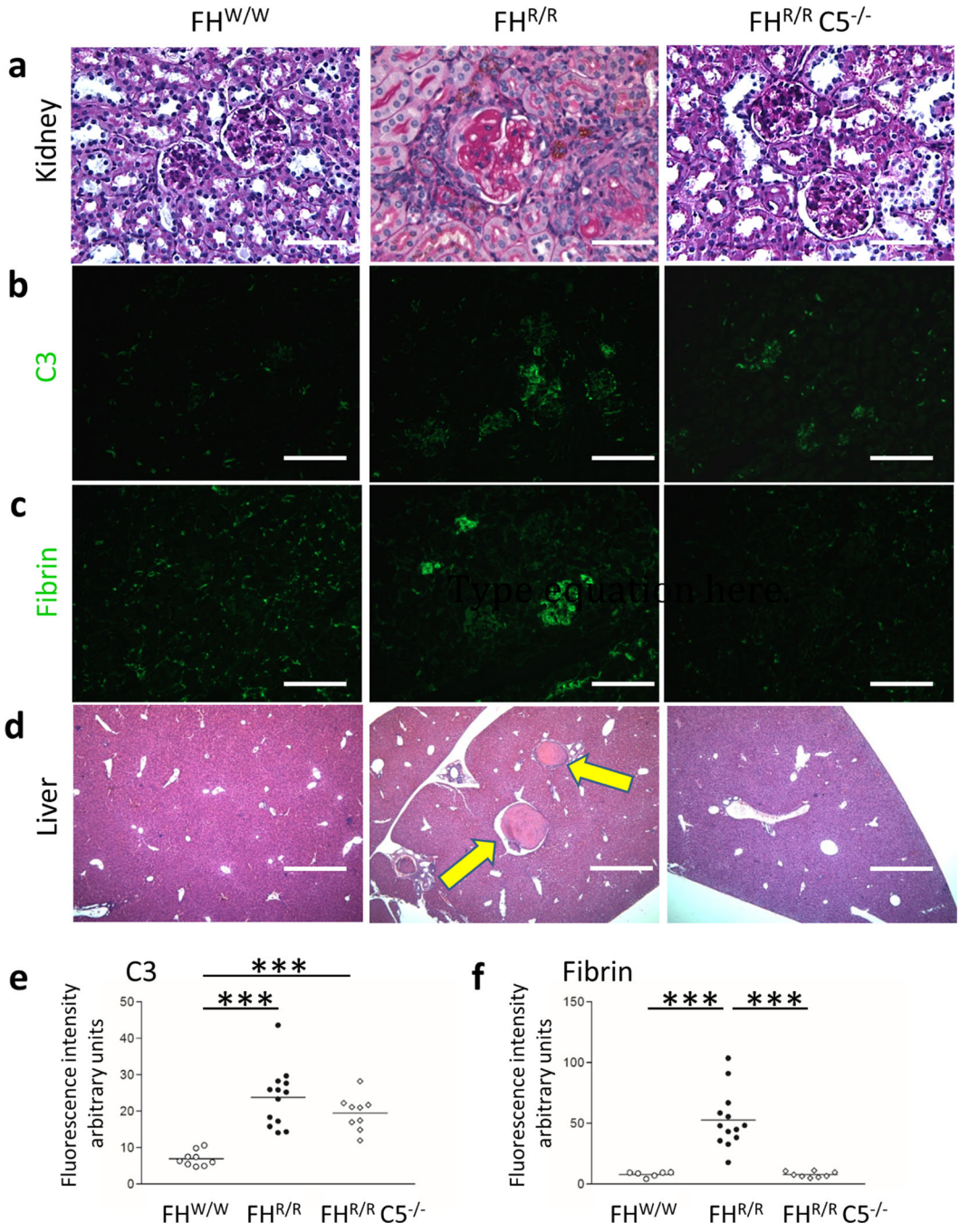


**Figure 2. C5 deficiency prevented renal TMA and liver thrombosis in $FH^{R/R}$ mice.**

(a) Representative histology of PAS-stained kidney sections from $FH^{W/W}$, $FH^{R/R}$ and $FH^{R/R}$ $C5^{-/-}$ mice (n = 10, 25 and 16 mice, respectively, were examined). $FH^{R/R}$ mouse kidney showed TMA features including arteriolar thrombosis, capillary wall thickening and double contours in glomeruli. Histology of $FH^{R/R}$ $C5^{-/-}$ mouse glomeruli was normal and similar to that of $FH^{W/W}$ mice. (b) Immunofluorescence staining showed C3 to be scanty within the $FH^{W/W}$ mouse glomeruli, but mesangial and capillary C3 staining of a granular pattern was observed in $FH^{R/R}$ and $FH^{R/R}$ $C5^{-/-}$ mice. (c) By immunofluorescence staining, fibrin

deposition was detected in the mesangial and capillary lesions of $FH^{R/R}$ mouse glomeruli but none was seen in $FH^{W/W}$ and $FH^{R/R}$ $C5^{-/-}$ mouse glomeruli. (d) Representative H&E staining of liver sections showing the presence of venous thrombi in $FH^{R/R}$ mice. No thrombus was observed in the liver of $FH^{W/W}$ and $FH^{R/R}$ $C5^{-/-}$ mice. (e, f) Quantitative analysis of glomerular C3 and fibrin immunofluorescence intensity. Both $FH^{R/R}$ and $FH^{R/R}$ $C5^{-/-}$ mice showed positive staining of glomerular C3 deposition but only $FH^{R/R}$ mice had fibrin deposition. In panels e and f, each dot represents the average value of multiple glomeruli on kidney sections of an individual mouse. Horizontal bars through scatter plots indicate average values from the groups of mice. ***$P < 0.001$. one-way ANOVA for panels e and f. Scale bars = 50 μm in panel a, 100 μm in panels b and c, and 25 μm in panel d.

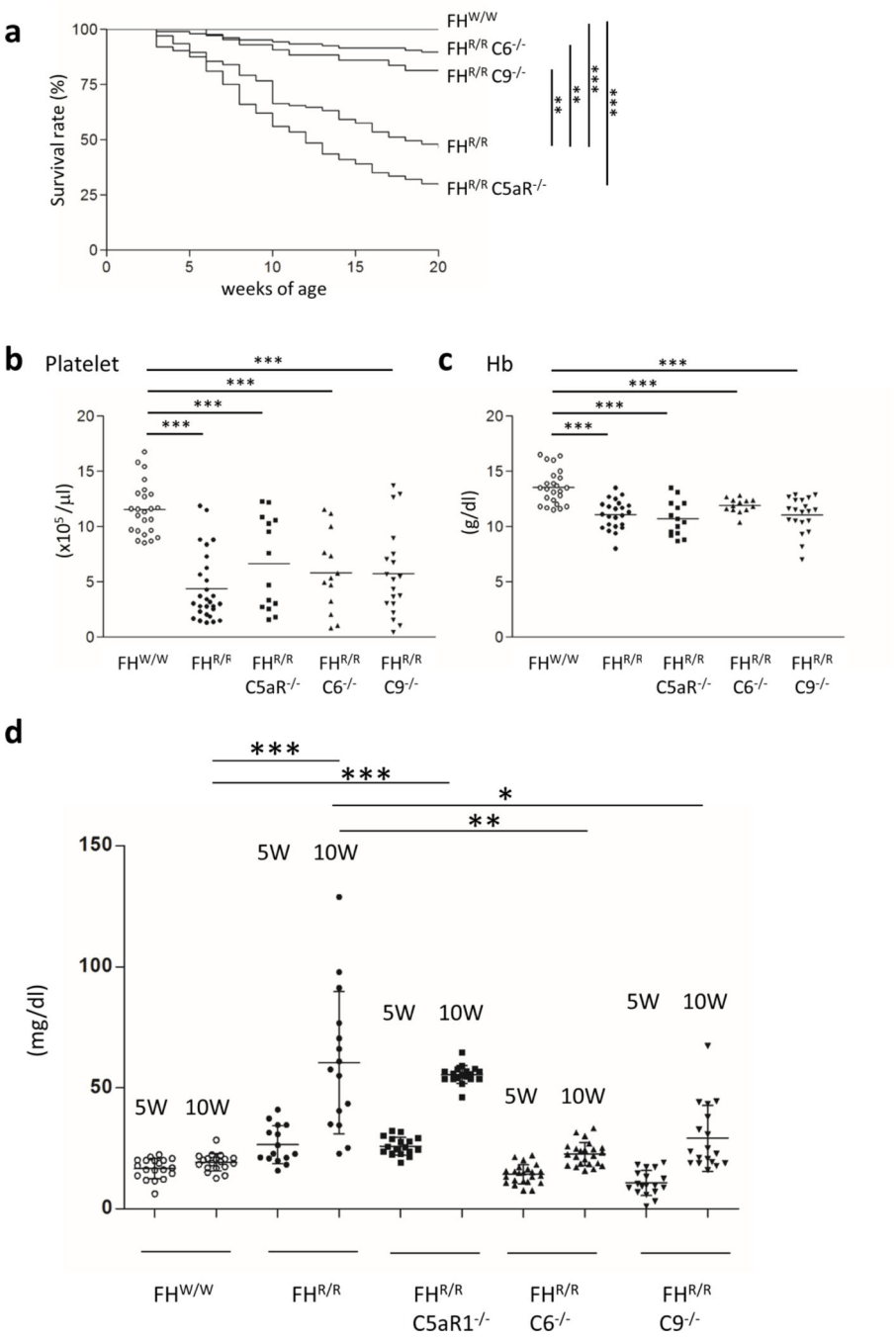


**Figure 3. Analysis of the effect of C5aR1, C6 or C9 deficiency on survival and aHUS phenotype of $FH^{R/R}$ mice.**

(a) 20-week survival curves of $FH^{W/W}$ (n = 50), $FH^{R/R}$ (n = 54), $FH^{R/R}$ $C5aR1^{-/-}$ (n = 66), $FH^{R/R}$ $C6^{-/-}$ (n = 60) and $FH^{R/R}$ $C9^{-/-}$ (n = 48) mice. Mortality was 0, 53.6 %, 70.5 %, 10.3 % and 18.6 %, respectively, for the above strains. (b-c) Neither C5aR1 nor C6 or C9 deficiency rescued the thrombocytopenia and anemia phenotype of $FH^{R/R}$ mice. Platelets and Hb were measured in 4–30 weeks old $FH^{W/W}$ (n = 24), $FH^{R/R}$ (n = 28), $FH^{R/R}$ $C5aR1^{-/-}$ (n = 14), $FH^{R/R}$ $C6^{-/-}$ (n = 13) and $FH^{R/R}$ $C9^{-/-}$ (n = 19) mice. Each dot represents the average of duplicate assays of an individual mouse. Horizontal bars through

scatterplots in panels b and c indicate the average values in each group. (d) BUN levels in $FH^{W/W}$ (n = 19), $FH^{R/R}$ (n = 15, $FH^{R/R}$ $C5aR1^{-/-}$ (n = 18), $FH^{R/R}$ $C6^{-/-}$ (n = 23) and $FH^{R/R}$ $C9^{-/-}$ (n = 18) mice measured at 5 weeks and 10 weeks of age. Only $FH^{R/R}$ and $FH^{R/R}$ $C5aR1^{-/-}$ mice had significantly elevated BUN at 10 weeks. There was also a trend of age-dependent BUN elevation in $FH^{R/R}$ $C9^{-/-}$ mice but it did not reach statistical significance. $*P < 0.05$, $**P < 0.01$, $***P < 0.001$. Mantel-Haeszel log-rank test for panel a, one-way ANOVA test for other panels.

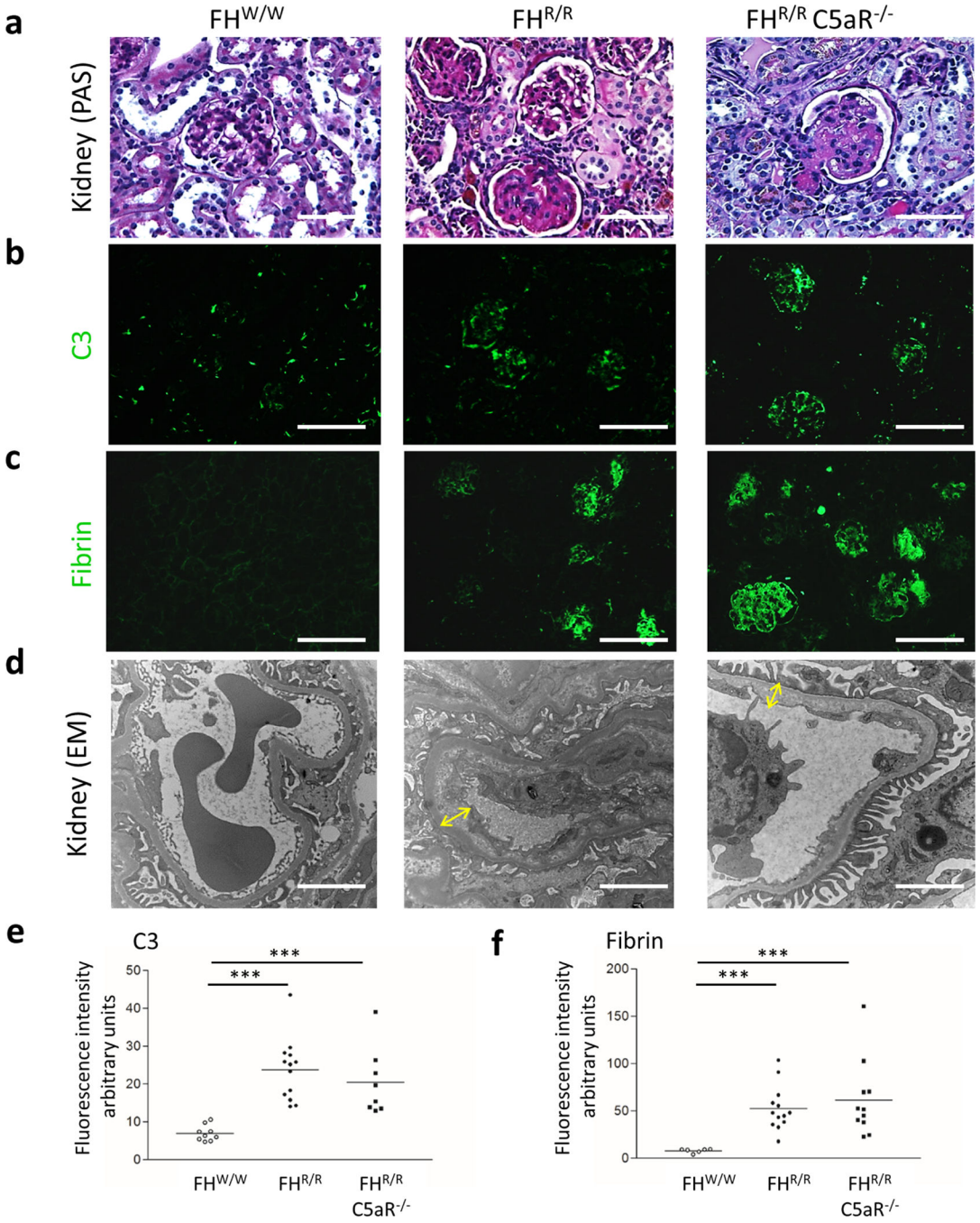


**Figure 4. C5aR1 deficiency did not prevent renal TMA pathology in $FH^{R/R}$ mice.**

(a) On light microscopy, both $FH^{R/R}$ and $FH^{R/R}$ $C5aR1^{-/-}$ mice exhibited TMA pathology in glomeruli. (b-c, e-f) Immunofluorescence staining showed similar glomerular C3 (b, e) and fibrin (c, f) deposition in $FH^{R/R}$ and $FH^{R/R}$ $C5aR1^{-/-}$ mice. (d) On electron microscopy, $FH^{W/W}$ mouse glomeruli had normal basement membrane and foot processes but both $FH^{R/R}$ and $FH^{R/R}$ $C5aR1^{-/-}$ mouse glomeruli showed characteristic TMA features including sub-endothelial space expansion (yellow arrow) and endothelial swelling without electron dense deposit. In panels e and f, each dot represents the average value of multiple glomeruli

of a given mouse. Horizontal bars through scatter plots indicate average values of mouse groups. *$P < 0.05$, **$P < 0.01$, ***$P < 0.001$. One-way ANOVA for panel e and f. Scale bars = 50 μm in panel a, 100 μm in panels b and c, and 2 μm in panel d.

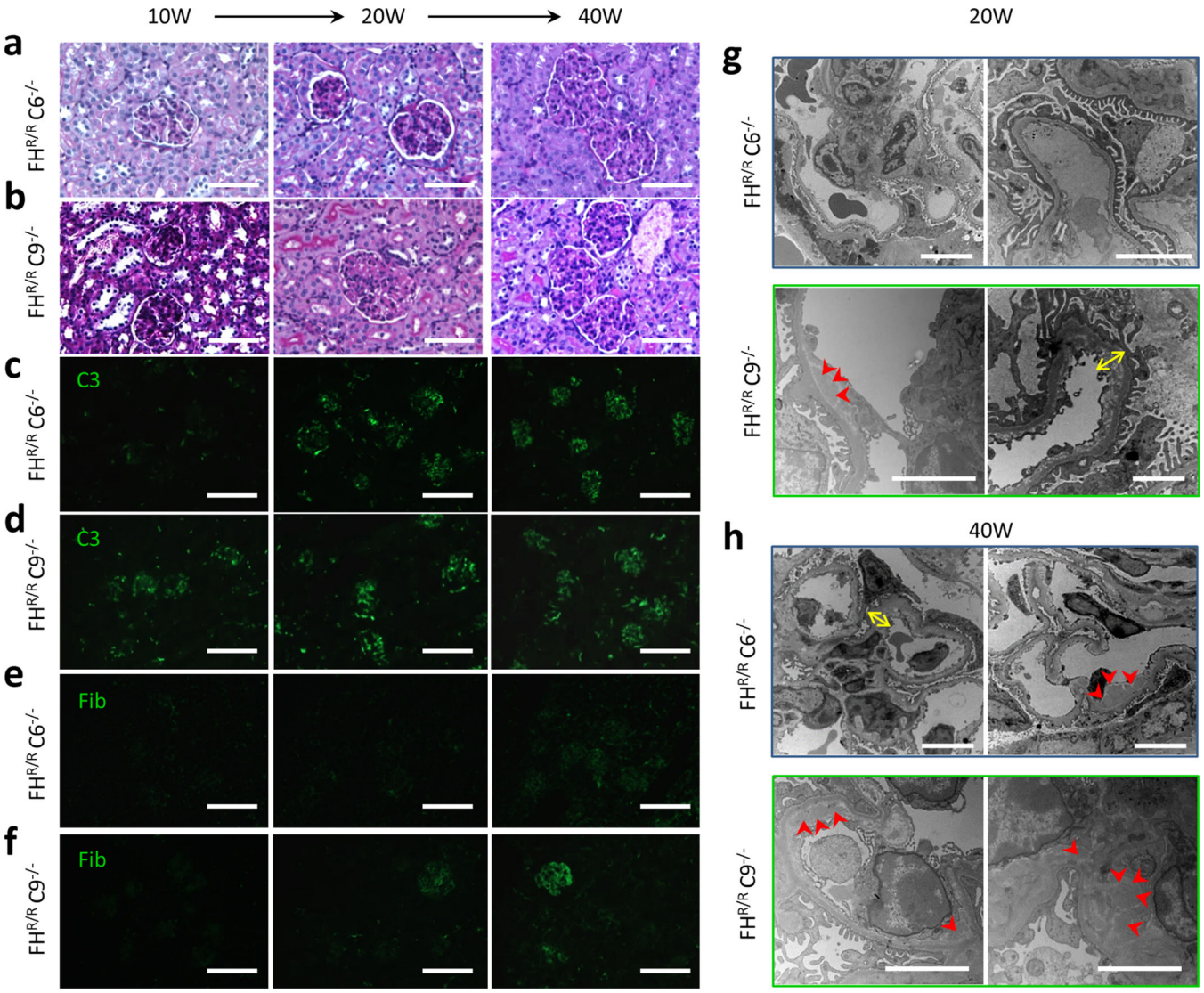


**Figure 5. Age-dependent changes in glomerular pathology of $FH^{R/R}$ $C6^{-/-}$ and $FH^{R/R}$ $C9^{-/-}$ mice.**

(a) $FH^{R/R}$ $C6^{-/-}$ mice showed mild and severe glomerular hypercellularity at 20 and 40 weeks of age, respectively, but few signs of TMA. (b) $FH^{R/R}$ $C9^{-/-}$ mice had glomerular hypercellularity at 10, 20 and 40 weeks, as well as glomerular micro-thrombi at 20 and 40 weeks of age. (c-d) Both $FH^{R/R}$ $C6^{-/-}$ and $FH^{R/R}$ $C9^{-/-}$ mice exhibited glomerular C3 deposition in capillary and mesangial lesions which was increased with age. (e-f) $FH^{R/R}$ $C9^{-/-}$ mice exhibited positive staining of fibrin in glomeruli at 20 and 40 weeks of age but none was detected the $FH^{R/R}$ $C6^{-/-}$ mouse glomeruli. (g) $FH^{R/R}$ $C6^{-/-}$ mouse glomeruli showed normal basement membrane and foot processes at 20 weeks of age but exhibited sub-endothelial space (yellow arrow) and electron-dense deposit in sub-endothelium (red arrow heads) at 40 weeks of age. (h) Sub-endothelial space expansion (yellow arrow) and dense deposits (red arrow heads) were found in $FH^{R/R}$ $C9^{-/-}$ mice both at 20 and 40 weeks of age. Scale bars = 50 μm in panels a and b, 100 μm in panels c-f, and 2 μm in panels g and h.

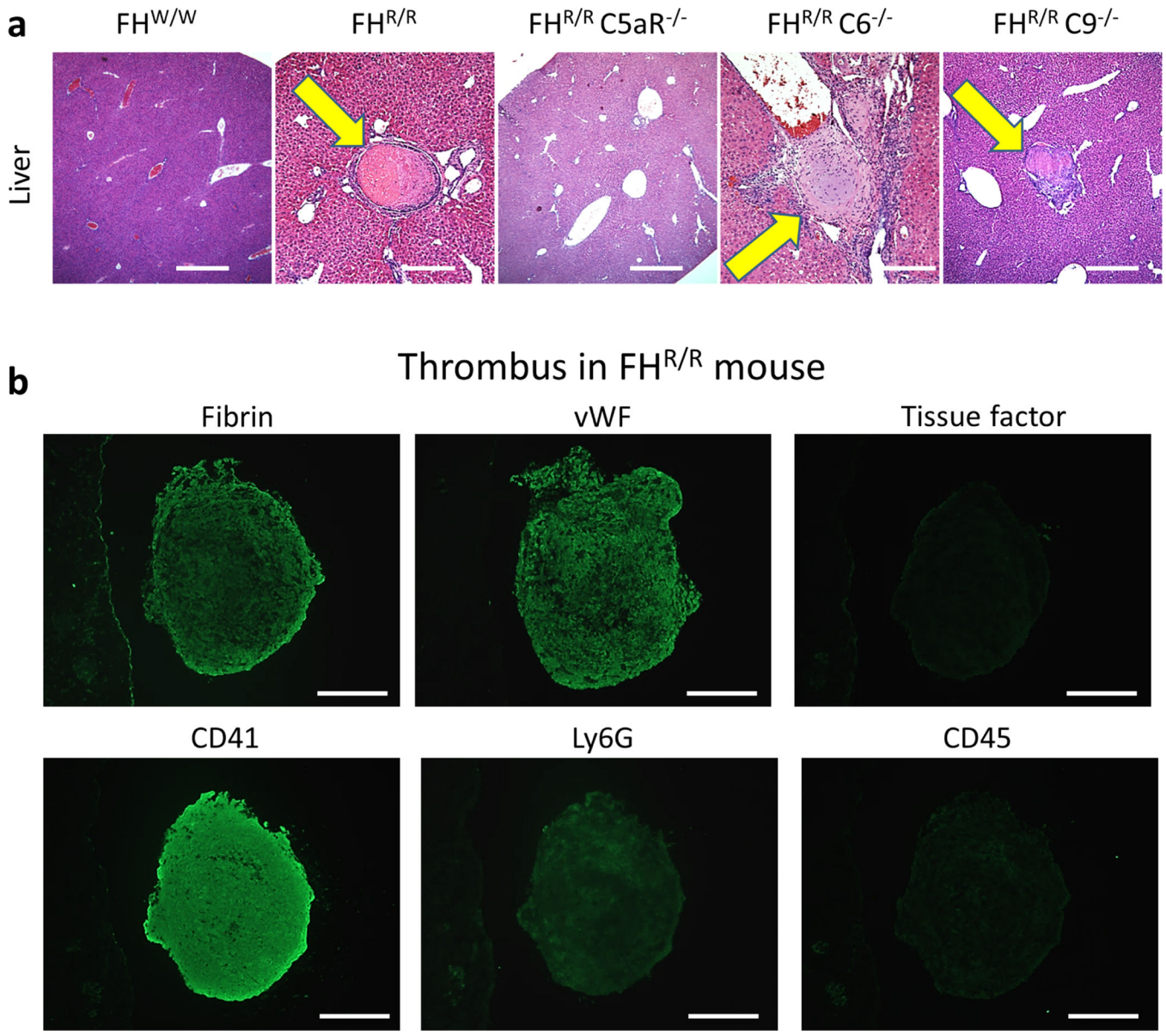


**Figure 6. Effect of C5aR1, C6 and C9 deficiency on macro-vessel thrombosis in $FH^{R/R}$ mice.**

(a) Venous thrombi (yellow arrow) was present in the liver of $FH^{R/R}$, $FH^{R/R}$ $C6^{-/-}$ and $FH^{R/R}$ $C9^{-/-}$ mice but not in the liver of $FH^{W/W}$ or $FH^{R/R}$ $C5aR1^{-/-}$ mice. (b) Immunofluorescence staining revealed the presence of vWF, fibrin, platelets (CD41) and neutrophils (Ly6G) in the liver thrombi of $FH^{R/R}$ mice. Weak staining for the leukocyte marker CD45 and no staining signal for tissue factor was detected in liver thrombi. Scale bars = 25 μm in panel a, and 100 μm in panel b.

**Table 1.**

**Glomerular pathology scoring and incidence of macro-vessel thrombosis in the kidney of all mouse strains and treatment groups.**

Number of mice examined in each group is listed at the bottom of the table. At least 3 different viewing fields in kidney sections (H&E and PAS staining) from each mouse were evaluated for 6 categories of kidney pathology as listed. All glomeruli on each section were examined and the percentage of glomeruli showing each pathological change was calculated. Mice were of mixed gender aged 4–40 weeks of age unless indicated otherwise.

| | Expanded matrix and endothelial swelling (%) | Micro-thrombi (%) | Large vein thrombi (%) | Glomerular sclerosis (%) | Arteriolar hyalinosis (%) | Glomerular hyper-cellularity (%) |
|---|---|---|---|---|---|---|
| FH $^{W/W}$ | 0 | 0 | 0 | 0 | 0 | 0 |
| FH $^{R/R}$ | 63.3 | 75.0 | 52.0 | 1.0 | 75.0 | 25.0 |
| FH $^{R/R}$ + anti-C5 Ab | 11.1 | 11.1 | 5.6 | 0.2 | 11.1 | 1.3 |
| FH $^{R/R}$ + control Ab | 48.0 | 87.5 | 50.0 | 0.3 | 87.5 | 30.0 |
| FH $^{R/R}$ C5$^{-/-}$ 4–20W | 0 | 0 | 0 | 0 | 0 | 0 |
| FH $^{R/R}$ C5 $^{-/-}$ 40W | 1.1 | 0 | 0 | 0 | 0 | 0 |
| FH $^{R/R}$ C5aR$^{-/-}$ | 45.7 | 66.7 | 0 | 0 | 66.7 | 28.3 |
| FH $^{R/R}$ C6 $^{-/-}$10W | 0 | 0 | 50.0 | 0 | 0 | 0 |
| FH $^{R/R}$ C6 $^{-/-}$20W | 0.1 | 0 | 75.0 | 0 | 0 | 8 |
| FH $^{R/R}$ C9 $^{-/-}$40W | 1.0 | 0 | 83.3 | 0 | 16.7 | 61.6 |
| FH $^{R/R}$ C9 $^{-/-}$10W | 1.7 | 14.3 | 75.0 | 0.1 | 14.3 | 72.9 |
| FH $^{R/R}$ C9 $^{-/-}$ 20W | 8.4 | 60.0 | 66.7 | 0.4 | 60.0 | 72.0 |
| FH $^{R/R}$ C9 $^{-/-}$40W | 40.0 | 75.0 | 100 | 0.5 | 66.7 | 84.5 |

(FH$^{W/W}$ $n$ = 10, FH$^{R/R}$ $n$ = 25, FH$^{R/R}$ + anti-C5 Ab $n$ = 16, FH$^{R/R}$ + control Ab $n$ = 20, FH$^{R/R}$ C5$^{-/-}$ 4–20W $n$ = 16, FH$^{R/R}$ C5$^{-/-}$ 40W $n$ = 7, FH$^{R/R}$ C5aR$^{-/-}$ $n$ = 12, FH$^{R/R}$ C6$^{-/-}$ 10W $n$ = 8 FH$^{R/R}$ C6$^{-/-}$ 20W $n$ = 8, FH$^{R/R}$ C6$^{-/-}$ 40W $n$ = 6, FH$^{R/R}$ C9$^{-/-}$ 10W $n$ = 8, FH$^{R/R}$ C9$^{-/-}$ 20W $n$ = 12, FH$^{R/R}$ C9$^{-/-}$ 40W $n$ = 6)

**Table 2.**

**Incidence of macro-vessel thrombosis in extra-renal sites of all mouse strains and treatment groups.**

At least 3 non-adjacent serial sections (H&E) from each mouse were 3 examined. Both the total number of mice studied and the number and percentage (in bracket) of 4 mice found to have macro-vessel thrombi are given.

| Phenotypes | $FH^{R/R}$ | $FH^{R/R}$ $C5^{-/-}$ | $FH^{R/R}$ + control Ab | $FH^{R/R}$ + anti C5 Ab | $FH^{R/R}$ $C5aR1^{-/-}$ | $FH^{R/R}$ $C6^{-/-}$ | $FH^{R/R}$ $C9^{-/-}$ |
|---|---|---|---|---|---|---|---|
| Brain thrombi | 4/25 (16) | 0/16 (0) | 2/20 (10) | 0/18 (0) | 0/18 (0) | 1/16 (6) | 1/13 (8) |
| Brain ischemic change | 14/25 (56) | 0/16 (0) | 4/20 (20) | 0/18 (0) | 2/18 (17) | 2/16 (13) | 0/13 (0) |
| Lung thrombi | 4/25 (16) | 0/16 (0) | 2/20 (10) | 0/18 (0) | 0/18 (0) | 5/16 (31) | 2/13 (15) |
| Heart thrombi | 2/25 (8) | 0/16 (0) | 0/20 (0) | 0/18 (0) | 0/18 (0) | 0/16 (0) | 0/13 (0) |
| Liver thrombi | 20/25 (80) | 0/16 (0) | 15/20 (75) | 0/18 (0) | 0/18 (0) | 10/16 (63) | 8/13 (62) |
| Spleen thrombi | 10/25 (40) | 0/16 (0) | 6/20 (30) | 0/18 (0) | 0/18 (0) | 5/16 (31) | 5/13 (39) |

(incidence (%), mixed gender, 4 – 20 weeks of age)